

1 **Quantifying SO₂ oxidation pathways to atmospheric sulfate by using**
2 **stable sulfur and oxygen isotopes: laboratory simulation and field**
3 **observation**

4 Ziyang Guo^a, Keding Lu^{a*}, Pengxiang Qiu^b, Mingyi Xu^b, Zhaobing Guo^{b*}

5
6 ^a State Key Joint Laboratory of Environmental Simulation and Pollution Control,
7 State Environmental Protection Key Laboratory of Atmospheric Ozone Pollution
8 Control, College of Environmental Sciences and Engineering, Peking University,
9 Beijing, China.

10 ^b Jiangsu Key Laboratory of Atmospheric Environment Monitoring and Pollution
11 Control (AEMPC), Collaborative Innovation Center of Atmospheric Environment and
12 Equipment Technology (CIC-AEET), School of Environmental Science and
13 Engineering, Nanjing University of Information Science and Technology, Nanjing
14 210044, China

15
16 * Correspondence to: k.lu@pku.edu.cn (Keding Lu), guocumt@nuist.edu.cn
17 (Zhaobing Guo)

19 **Abstract.** The formation of secondary sulfate in the atmosphere remains controversial, and it is urgent
20 to seek for a new method to quantify different sulfate formation pathways. Thus, SO₂ and PM_{2.5}
21 samples were collected from 4 to 22 Dec. 2019 in Nanjing region. Sulfur and oxygen isotopic
22 compositions were synchronously measured to study the contribution of SO₂ homogeneous and
23 heterogeneous oxidation to sulfate. Meanwhile, the correlation of δ¹⁸O values between H₂O and sulfate
24 from SO₂ oxidation by H₂O₂ and Fe³⁺/O₂ were simulatively investigated in the laboratory. Based on
25 isotope mass equilibrium equations, the ratios of different SO₂ oxidation pathways were quantified. The
26 results showed that secondary sulfate constituted higher than 80% of total sulfate in PM_{2.5} during the
27 sampling period. Laboratory simulation experiments indicated that δ¹⁸O value of sulfate was linearly
28 dependent on δ¹⁸O value of water, and the slopes of linear curves for SO₂ oxidation by H₂O₂ and
29 Fe³⁺/O₂ were 0.43 and 0.65, respectively. The secondary sulfate in PM_{2.5} was mainly ascribed to SO₂
30 homogeneous oxidation by OH radicals and heterogeneous oxidation by H₂O₂ and Fe³⁺/O₂. SO₂
31 heterogeneous oxidation was generally dominant during sulfate formation, and SO₂ oxidation by H₂O₂
32 predominated in SO₂ heterogeneous oxidation reactions with an average ratio around 54.6%. This study
33 provided an insight into precisely evaluating sulfate formation by combining stable sulfur and oxygen
34 isotopes.

35
36
37
38
39
40

41 **1 Introduction**

42 Sulfate is one of the prevalent components of PM_{2.5} (Briggemann et al., 2021; Huang et al., 2014;
43 Yang et al., 2023). Sulfate makes up approximately 25% of PM_{2.5} mass in Shanghai, 23% in
44 Guangzhou and 10-33% in Beijing (Xue et al., 2016). The rapid sulfate formation is a crucial factor
45 determining the explosive growth of fine particles and the frequent occurrence of severe haze events in
46 China (Lin et al., 2022; Liu et al., 2020; Meng et al., 2023; Wang et al., 2021). Sulfate plays an
47 important role in the chemical and physical processes in the troposphere and lower stratosphere, which
48 significantly affects global climate change by scattering solar radiation and acting as cloud
49 condensation nuclei (Gao et al., 2022; Ramanathan et al., 2001). Meanwhile, sulfate exerts a significant
50 influence on air quality and public health (Abbatt et al., 2006).

51 In the past decades, numerous attempts have been made to evaluate SO₂ oxidation pathways
52 involving in homogeneous and heterogeneous reactions. Traditionally, sulfate formation mechanisms
53 mainly include SO₂ homogeneous oxidation by OH radicals and heterogeneous oxidation by H₂O₂, O₃
54 and O₂ catalyzed by transition metal ions (TMIs) in cloud/fog water droplets. The relative importance
55 of different sulfate formation pathways is strongly dependent on oxidant concentrations, occurrence of
56 fog/cloud events and pH of aqueous phase (Kuang et al., 2022; Oh et al., 2023). Generally, SO₂
57 homogeneous oxidation by OH radicals and heterogeneous oxidation by H₂O₂ are considered the most
58 important pathways for sulfate production on the global scale (Seinfeld and Pandis, 1998). The
59 photochemical reactivity during the winter in Beijing has been found to be relatively high, which
60 favored the formation of reactive species such as OH radicals and H₂O₂, thereby facilitating SO₂
61 oxidation (Zhang et al., 2020). Xue et al. (2014) suggested that SO₂ oxidation by O₃ and H₂O₂ in
62 aqueous phase contributed to the majority of total sulfate production. Liu et al. (2020) proposed that
63 S(IV) oxidation by H₂O₂ in aerosol water could be an important pathway considering the ionic strength
64 effect. He et al. (2018) found that the contribution of SO₂ oxidation by H₂O₂ could reach 88% during
65 Beijing haze period. Ye et al. (2018) observed that SO₂ oxidation rate by H₂O₂ was 2-5 times faster
66 than the summed rate of the other three oxidation pathways. As a result, actual contribution of SO₂
67 oxidation by H₂O₂ during the winter might be underestimated in the previous studies.

68 In addition, the presence of NO₂ was obviously favorable for SO₂ oxidation under the conditions of
69 high [relative humidity \(RH\)](#) and NH₃. NH₃ can promote the hydrolysis of NO₂ dimers to HONO and

70 result in more sulfate formation on particle surface in humid conditions. However, this conclusion was
71 doubted by Liu et al. (2017) who believed that the reaction on actual fine particles with pH at 4.2 was
72 too slow to account for sulfate formation. Li et al. (2020) deemed that SO₂ oxidation by NO₂ might not
73 be a major oxidation pathway in China. Furthermore, GEOS-Chem modeling study suggested that NO₂
74 oxidation contributed less than 2% of total sulfate production. It is found that TMI pathway was very
75 important in highly polluted regions, and the contribution of metal-catalyzed SO₂ oxidation to sulfate
76 was as high as 49±10% in haze. Wang et al. (2021) also argued that SO₂ oxidation via TMI on aerosol
77 surface could be the dominant sulfate formation pathway. They found that manganese-catalyzed
78 oxidation of SO₂ contributed 69.2±5.0% in sulfate production. Overall, the mechanisms for sulfate
79 rapid growth remain unclear and controversial. Therefore, sulfate formation pathways need to be
80 further explored, and it is urgent to develop a new method to quantify different sulfate formation
81 processes.

82 Generally, sulfur isotopes allow for investigating SO₂ oxidation processes in the atmosphere because
83 of distinctive isotope fractionation associated with different oxidation reactions (Harris et al., 2013).
84 Harris et al. (2012) presented [the respective](#) sulfur isotope fractionation factors of SO₂ oxidation by OH,
85 O₃/H₂O₂ and iron catalysis ~~were 1.0087, 1.0167 and 0.9905, respectively.~~ Besides, the observed sulfur
86 isotope fractionation of SO₂ oxidation by H₂O₂ and O₃ appeared to be no significant difference.
87 Therefore, the results were particularly useful to determine the importance of transition metal-catalyzed
88 oxidation pathway compared to other oxidation pathways. However, other main SO₂ oxidation
89 pathways could not be distinguished only based on stable sulfur isotope determination.

90 Oxygen isotope ratio (δ¹⁸O) can be used to deduce sulfate formation processes due to those SO₂
91 oxidation pathways affect oxygen isotope of product sulfate differently. Especially, mass-independent
92 fractionation signals of oxygen isotopes (nonzero Δ¹⁷O, where Δ¹⁷O=δ¹⁸O-0.52×δ¹⁷O) in sulfate are
93 usually adopted to investigate the contribution of different SO₂ oxidation pathways. This method can
94 identify the contribution of SO₂+O₃ pathway when high Δ¹⁷O value (>3‰) is measured in sulfate.
95 However, there is presence of obvious uncertainty when interpreting the sulfate with low Δ¹⁷O value
96 (<1‰). Unfortunately, most sulfate samples in the atmosphere present Δ¹⁷O<1‰, suggesting a limited
97 contribution of SO₂+O₃ pathway during sulfate formation. It is noteworthy that the contribution of
98 SO₂+H₂O₂ and TMI pathway is unclear if solely using Δ¹⁷O (Li et al., 2020). Holt and Kumar (1984)

带格式的: 字体: (默认) Times New Roman, 10 磅, 字体颜色: 自动设置, 图案: 清除

带格式的: 字体颜色: 自动设置

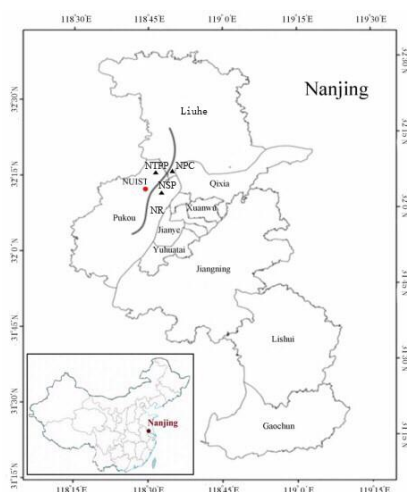
99 found oxygen isotope was a valuable and complementary method to determine probable mechanisms of
100 SO₂ oxidation to sulfate in the atmosphere. This provides us an insight into precisely evaluating sulfate
101 formation pathways by combining oxygen and sulfur isotopes.

102 In this contribution, PM_{2.5} and SO₂ were sampled from 4 to 22 Dec. 2019 in Nanjing. Sulfur and
103 oxygen isotopic compositions were measured to study the contribution of SO₂ homogeneous and
104 heterogeneous oxidation during sulfate formation. In addition, the linear relationships of δ¹⁸O values
105 between H₂O and sulfate from SO₂ oxidation by H₂O₂ and Fe³⁺/O₂ were synchronously investigated in
106 the laboratory. Based on sulfur and oxygen isotopes mass equilibrium equations, the ratios of different
107 SO₂ oxidation pathways during the sampling period were calculated. The study aims to seek for a novel
108 method to quantify different SO₂ oxidation processes with sulfur and oxygen isotopes.

109 2 Materials and methods

110 2.1 Sampling location

111 PM_{2.5} and SO₂ in the atmosphere were sampled from 4 to 22 Dec. 2019 in Nanjing, China. The
112 sampling site was located at the roof of the library in Nanjing University of Information Science &
113 Technology (NUIST, 32.1 °N, 118.5 °E), which is depicted in Fig. 1. The sampling location is at the
114 side of Ningliu Road and closely next to Nanjing chemical industry park. There is presence of some
115 large-scale chemical enterprises such as Nanjing steel plant, Nanjing thermal power plants and Nanjing
116 petrochemical company, which inevitably release lots of SO₂ and iron metal into the atmosphere.



117
118 Fig. 1. Sampling site of NUIST in Nanjing, China. NSP: Nanjing steel plants; NTPP: Nanjing

119 thermal power plants; NPC: Nanjing petrochemical company; NR: Ningliu Road.

120 2.2 PM_{2.5} and SO₂ Samples collection

121 PM_{2.5} and SO₂ were sampled by using a modified JCH-1000 sampler (Juchuang Co., Qingdao) with
122 a flow rate of 1.05 m³ min⁻¹ from 8 am to 8 pm from 4 to 22 Dec. 2019. PM_{2.5} and SO₂ were collected
123 with quartz filter (203×254 mm, Munktell, Sweden) and glass fiber filter (203×254 mm, Tisch
124 Environment INC, USA), respectively. The filters were incinerated in a muffle furnace at 450 °C for 2h
125 and then preserved in the desiccators at room temperature. The glass fiber filters were firstly soaked in
126 2% K₂CO₃ and 2% glycerol solution for 2h and dried in DGG-9070A electric oven. SO₂ can be
127 changed into sulfite immediately during the sampling.

128 2.3 Extractions of water-soluble sulfate

129 PM_{2.5} sample filters were shredded and soaked in 400 mL of Milli-Q (18 MΩ) water for extractions
130 of water-soluble sulfate. Filters were then isolated from solutions by centrifugation and sulfate was
131 precipitated as BaSO₄ by adding 1 mol L⁻¹ BaCl₂. After the filtration with 0.22 μm acetate membrane,
132 BaSO₄ precipitate was rinsed with Milli-Q water to remove Cl⁻. Finally, BaSO₄ powders were calcined
133 at 800 °C for 2h to obtain high purity BaSO₄. In addition, a small amount of H₂O₂ solution was added
134 to oxidize sulfite to sulfate.

135 2.4 Laboratory simulation of SO₂ oxidation by H₂O₂ and Fe³⁺/O₂

136 For SO₂ oxidation by H₂O₂, 30 mL min⁻¹ Ar was firstly introduced into three kinds of different water
137 about 30 min to drive out air. Sulfate was produced by adding 10 mL H₂O₂ dilute solution (0.1 mL 30%
138 H₂O₂ in 50 mL water) to SO₂ in the reaction chamber at 10 °C. H₂O₂ solution was agitated vigorously
139 for 1min before admission of air. For SO₂ oxidation by Fe³⁺/O₂, 2 mL min⁻¹ SO₂ and 2 mL min⁻¹ O₂
140 were simultaneously put into Fe³⁺ dilute solution at 10 °C. Then, 10 mL 1 mL min⁻¹ BaCl₂ was added to
141 prepare BaSO₄. Oxygen isotopic compositions of product sulfate and three kinds of water were
142 measured to study their linear relationships.

143 2.5 Sulfur and oxygen isotope determination

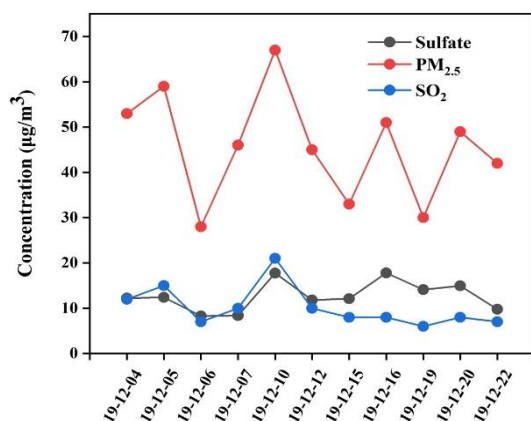
144 Sulfur isotopic compositions in sulfate were analyzed using Elemental analyzer (EA, Flash 2000,
145 Thermo) and isotope mass spectrometer (IRMS, Delta V Plus, Finningan). High-purity BaSO₄ was
146 converted into SO₂ in EA in the presence of Cu₂O. SO₂ from EA was ionized and δ³⁴S value was

147 measured using IRMS. For the determination of $\delta^{18}\text{O}$, BaSO_4 pyrolysis was conducted in graphite
 148 furnace at 1450 °C, and $\delta^{18}\text{O}$ value was obtained in CO produced from the pyrolysis at continuous-flow
 149 mode. The results of $\delta^{34}\text{S}$ and $\delta^{18}\text{O}$ were with respect to international standard V-CDT and V-SMOW,
 150 and the accuracy were better than $\pm 0.2\%$ and $\pm 0.3\%$, respectively.

151 3 Results and discussion

152 3.1 Concentrations of $\text{PM}_{2.5}$, sulfate and SO_2

153 As described in Fig. 2, the mass concentrations of $\text{PM}_{2.5}$, SO_4^{2-} and SO_2 during the period from 4 to
 154 22 Dec. 2019 in NUIST changed from 28.1 to 67.0 $\mu\text{g m}^{-3}$, 8.3 to 17.8 $\mu\text{g m}^{-3}$ and 6.2 to 20.9 $\mu\text{g m}^{-3}$
 155 with an average and standard deviation at $45.7 \pm 12.1 \mu\text{g m}^{-3}$, $12.7 \pm 3.3 \mu\text{g m}^{-3}$ and $10.2 \pm 4.4 \mu\text{g m}^{-3}$,
 156 respectively. It can be observed that $\text{PM}_{2.5}$ average concentration was about 1.3 times of the First Grade
 157 National Ambient Air Quality Standard ($35 \mu\text{g m}^{-3}$) and beyond the safety standard of World Health
 158 Organization ($10 \mu\text{g m}^{-3}$). The photochemical reactivity during the winter in Beijing has been found to
 159 be relatively high (Zhang et al., 2020), which facilitates the formation of some photooxidants. The
 160 relatively clean days during the sampling period indicates the importance of photoinduced oxidation of
 161 SO_2 .



162
 163 **Fig. 2. Variations in concentrations of $\text{PM}_{2.5}$, SO_4^{2-} and SO_2 .**

164 Meanwhile, the change trends of $\text{PM}_{2.5}$, SO_4^{2-} and SO_2 concentrations were found to be basically the
 165 same during the sampling period, indicating sulfate was mainly from SO_2 oxidation. Especially, $\text{PM}_{2.5}$,
 166 SO_4^{2-} and SO_2 concentrations increased to the maximum values on 10 Dec.. It is noted that NO_2 and

带格式的: 下标

带格式的: 下标

带格式的: 上标

带格式的: 下标

167 CO concentrations were 85 and 1.60 $\mu\text{g m}^{-3}$ on 10 Dec., which were also the maximum values during
168 the sampling period. Based on the wind speed was lower than 3m s^{-1} , and there was presence of static
169 weather during the sampling period, we believed that high CO concentration was mainly from local
170 emissions. However, O_3 concentration on 10 Dec. was the minimum value at $24 \mu\text{g m}^{-3}$, which
171 preliminarily indicated that SO_2 oxidation by NO_2 might be a major pathway in sulfate formation.
172 Previous studies showed that SO_2 oxidation by NO_2 in aerosol water dominated heterogeneous sulfate
173 formation during wintertime at neutral aerosol pH (Wang et al., 2016; Cheng et al., 2016). However,
174 subsequent studies showed that the calculated aerosol pH was in the range of 4.2~4.7, and the
175 reactions between SO_2 and NO_2 during this pH range were too slow to produce sulfate. Taking into
176 account low aerosol pH in Nanjing region, we suggested that SO_2 oxidation by NO_2 was not a
177 dominant pathway for sulfate formation during the sampling period.

178 In contrast, $\text{PM}_{2.5}$, SO_4^{2-} and SO_2 concentrations were observed to be at the minimum values on 6
179 Dec.. Similarly, NO_2 and CO concentrations were also at the minimum of 36 and 0.6mg m^{-3} ,
180 respectively. However, O_3 concentration on 6 Dec. was the maximum at $50 \mu\text{g m}^{-3}$. Besides, the rate of
181 SO_2 oxidation with O_3 becomes fast only when $\text{pH}>5$, the reaction rate of SO_2 with O_3 is one hundredth
182 of those with H_2O_2 or TMI when $\text{pH}<5$. Therefore, pH values of actual fine particles at 4~5 in Nanjing
183 region could markedly restrain SO_2 oxidation by O_3 . The lowest SO_4^{2-} concentration on 6 Dec. further
184 demonstrated that SO_2 oxidation by O_3 played an insignificant role in sulfate formation.

185 Generally, aqueous-phase oxidation is deemed to be a main process of sulfate formation in
186 atmospheric environment. Shao et al. (2018) believed that heterogeneous sulfate production on aerosols
187 occurred when ~~relative humidity (RH)~~ was higher than 50 %. The RH values of the atmosphere ranging
188 from 50.7 to 88.9% during the sampling period indicated that sulfate formation was closely related to
189 SO_2 heterogeneous oxidation.

190 3.2 Sulfur isotopic compositions in sulfate and SO_2

191 It can be observed from Fig. 3 that the values of $\delta^{34}\text{S-SO}_4^{2-}$ were generally higher compared to those
192 of $\delta^{34}\text{S-SO}_2$ during the sampling period except that on 16 Dec.. The $\delta^{34}\text{S-SO}_4^{2-}$ values ranged from 3.1
193 to 4.7‰ with an average and standard deviation at $4.0\pm 0.6\%$, while $\delta^{34}\text{S-SO}_2$ values changed from -2.9
194 to 4.7‰ with an average and standard deviation at $-0.2\pm 2.3\%$. The discrepancy between the values of
195 $\delta^{34}\text{S-SO}_4^{2-}$ and $\delta^{34}\text{S-SO}_2$ was mainly related to sulfur isotope fractionation effect during SO_2 oxidation

带格式的: 字体: (中文) 宋体, 10 磅

带格式的: 字体: (中文) 宋体, 10 磅

带格式的: 字体: (中文) 宋体, 10 磅

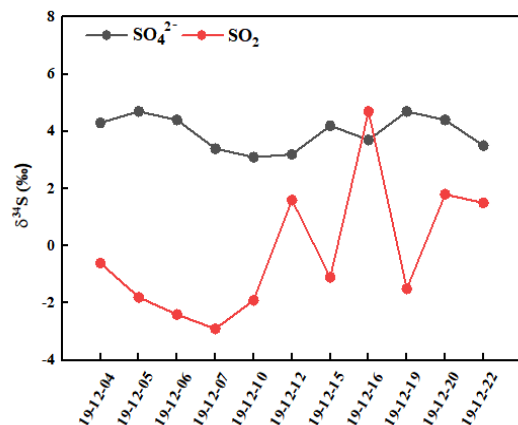
带格式的: 上标

带格式的: 字体: (中文) 宋体, 10 磅

带格式的: 字体: (中文) 宋体, 10 磅

带格式的: 字体颜色: 红色

196 to secondary sulfate.

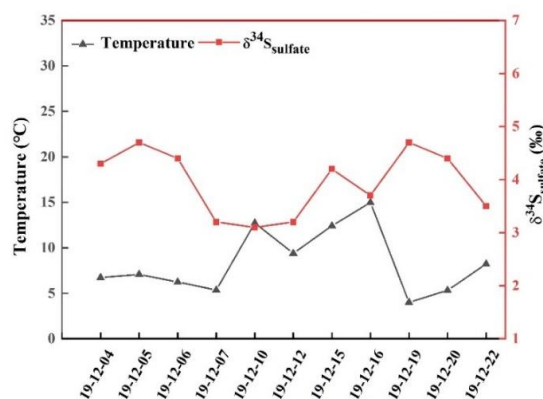


197
198 **Fig. 3. Variations in sulfur isotopic compositions in sulfate and SO₂**

带格式的: 下标

199 It is noteworthy that $\delta^{34}\text{S-SO}_4^{2-}$ values were similar to that in $\text{PM}_{2.5}$ with an average at 4.2‰ during
200 Youth Olympic Games in Aug. 2014 in Nanjing (Guo et al., 2016). However, the average value of
201 $\delta^{34}\text{S-SO}_4^{2-}$ during the sampling period was lower than 5.6‰ in Nanjing during a typical haze event
202 from 21 Dec. 2015 to 1 Jan. 2016 (Guo et al., 2019). The higher $\delta^{34}\text{S}$ values of sulfate in haze was
203 possibly ascribed to SO_2 heterogeneous oxidation, which typically enriched heavy sulfur isotope in
204 sulfate. In this study, the average concentrations of $\text{PM}_{2.5}$ was $45.7 \mu\text{g m}^{-3}$, indicating a not heavily
205 polluted time interval. Besides, the relatively high temperature during the sampling period was
206 favorable for photochemical reactions and OH radicals' formation. As a result, the contribution of SO_2
207 homogenous oxidation increased during sulfate formation, which enriched light sulfur isotope
208 compared to that in haze. Han et al. (2017) determined $\delta^{34}\text{S}$ values in Beijing $\text{PM}_{2.5}$ with an average at
209 6.0‰. It is observed that there existed a regional difference in $\delta^{34}\text{S-SO}_4^{2-}$ values. The $\delta^{34}\text{S-SO}_4^{2-}$ value
210 in Nanjing was generally lower than that in Beijing. The discrepancy of $\delta^{34}\text{S-SO}_4^{2-}$ value illustrated
211 different sulfur sources and SO_2 oxidation pathways in these regions. In addition, $\delta^{34}\text{S-SO}_4^{2-}$ values
212 presented a seasonal change. $\delta^{34}\text{S}$ values in Beijing aerosol sulfate varied from 3.4 to 7.0‰ with a
213 average of 5.0‰ in summer and from 7.1 to 11.3‰ with an average of 8.6‰ in winter. Generally, SO_2
214 homogeneous oxidation dominated in summer compared to that in winter due to strong solar irradiation
215 (Han et al., 2016). SO_2 oxidation might lead to sulfur isotope fractionation, which was mainly
216 attributed to equilibrium or kinetic discrimination between SO_2 and sulfate. The influence of different
217 oxidants on sulfur isotope fractionation needed to be further investigated.

218 Fig.4 presents the relationship between $\delta^{34}\text{S}\text{-SO}_4^{2-}$ value and atmospheric temperature during the
 219 sampling period. It can be observed that there existed an obviously negative correlation. The higher
 220 temperature generally corresponded to the lower $\delta^{34}\text{S}\text{-SO}_4^{2-}$ value. This is mainly ascribed to kinetic
 221 effect of sulfur isotope fractionation during SO_2 oxidation. At high temperature, more OH radicals were
 222 produced and the contribution of SO_2 homogeneous oxidation increased. It is reported that sulfur
 223 isotope fractionation about SO_2 was -9‰ for homogeneous oxidation process (Tanaka et al., 1994).
 224 Therefore, low $\delta^{34}\text{S}$ value in sulfate at high temperature was chiefly due to elevated SO_2 homogeneous
 225 oxidation.



226
 227 **Fig. 4.** The correlation between $\delta^{34}\text{S}\text{-SO}_4^{2-}$ value and atmospheric temperature.

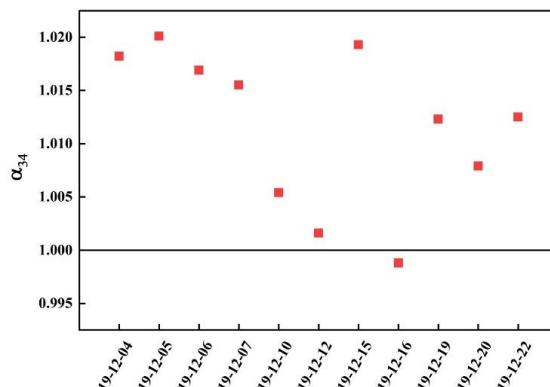
228 3.3 Sulfur isotope fractionation during SO_2 oxidation

229 The secondary sulfate was generally from SO_2 homogeneous and heterogeneous oxidation (Seinfeld
 230 and Pandis, 1998). The homogeneous and heterogeneous oxidation of SO_2 might lead to sulfur isotope
 231 fractionation, which is described by using fractionation coefficient (α)

$$\alpha = \frac{\frac{\delta^{34}\text{S}_{\text{SO}_4^{2-}}}{10^3} + 1}{\frac{\delta^{34}\text{S}_{\text{SO}_2} + 1}{10^3}} \quad (1)$$

232
 233 Sulfate enriched heavy sulfur isotope ($\alpha > 1$) during SO_2 heterogeneous oxidation for the presence of
 234 isotope equilibrium fractionation and kinetic fractionation. However, sulfate enriched light sulfur
 235 isotope ($\alpha < 1$) during SO_2 homogeneous oxidation due to this process was only related to kinetic
 236 fractionation. As described in Fig. 5, α values ranged from 0.9988 to 1.0201 indicating there existed
 237 SO_2 homogeneous and heterogeneous oxidation during the sampling period. α value was at the

238 minimum of 0.9988 on 16 Dec., which showed SO₂ homogeneous oxidation played a crucial role.



239

240 **Fig. 5.** Sulfur isotope fractionation coefficients during SO₂ oxidation.

241 It is reported that sulfur isotope fractionations during SO₂ heterogeneous and homogeneous oxidation
242 to sulfate were 16.5‰ and -9‰, respectively (Tanaka et al., 1994). Consequently, the contribution of
243 SO₂ heterogeneous and homogeneous oxidation to sulfate could be calculated by sulfur isotope mass
244 equilibrium equations (2) and (3).

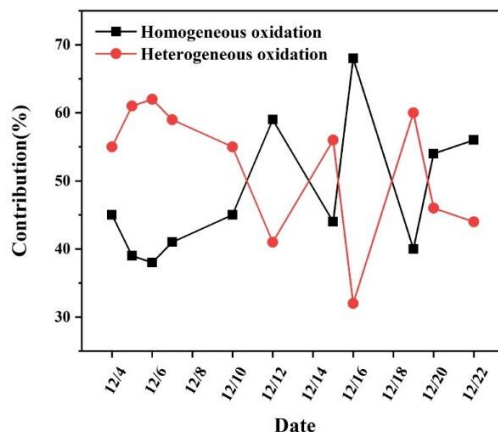
$$245 \quad \delta^{34}\text{S}_{\text{SO}_2} + 16.5x - 9y = \delta^{34}\text{S}_{\text{SO}_4^{2-}} \quad (2)$$

$$246 \quad x + y = 1 \quad (3)$$

247 where x and y represent the contribution of SO₂ heterogeneous and homogeneous oxidation,
248 respectively.

249 It is observed from Fig. 6 that most of the days (7 out of 11) had more than 50% contributions from
250 SO₂ heterogeneous oxidation, contribution of SO₂ heterogeneous oxidation markedly fluctuated ranging
251 from 31.4 to 62.0% with an average and standard deviation at 51.6 ± 0.1%, which indicated that SO₂
252 heterogeneous oxidation was generally dominant during sulfate formation. He et al. (2018) presented
253 the observations of oxygen-17 excess of PM_{2.5} sulfate collected in Beijing haze from Oct. 2014 to Jan.
254 2015, and found the contribution of heterogeneous sulfate production was about 41~54% with a mean
255 of 48 ± 5%. The contribution of SO₂ heterogeneous oxidation reached high-level during 5-7 Dec. and on
256 19 Dec., which was closely related to the temperature of the atmosphere. The low temperature about
257 5°C during these days was favorable for SO₂ dissolution in water and further oxidized to sulfate. On 16
258 Dec., the contribution of SO₂ heterogeneous oxidation was at the minimum of 31.4%. The highest
259 temperature of 15°C on 16 Dec. restrained SO₂ solubility in aqueous solution and produced lots of

260 gaseous oxidants such as OH radicals to promote SO₂ homogeneous oxidation.



261

262 **Fig. 6.** The contributions of SO₂ heterogeneous and homogeneous oxidation to sulfate.

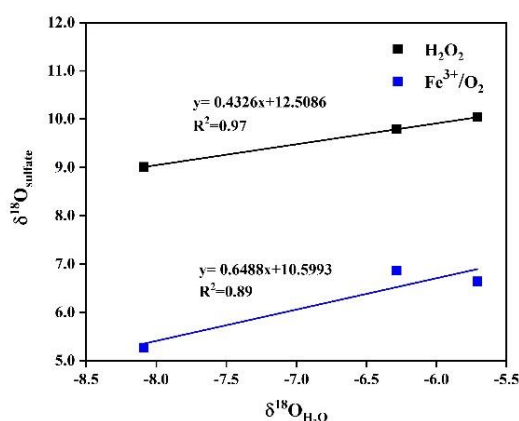
263 Overall, the temperature was an important factor in controlling SO₂ oxidation pathways. High
264 temperature facilitated kinetic fractionation of sulfur isotope during SO₂ oxidation to sulfate, thereby
265 decreasing $\delta^{34}\text{S}$ value in sulfate. In addition, there was lack of positive correlation between the
266 contribution of SO₂ heterogeneous oxidation and O₃ or NO₂ concentration. This further demonstrated
267 that SO₂ oxidation by O₃ and NO₂ were not the important pathways during the sampling period.
268 Consequently, we mainly focused on SO₂ heterogeneous oxidation by H₂O₂ and Fe³⁺/O₂ in the
269 following study.

270 3.4 The correlation of $\delta^{18}\text{O}$ values between H₂O and SO₄²⁻ from SO₂ oxidation by H₂O₂ and Fe³⁺/O₂

271 It is known that SO₂ rapidly equilibrates with ambient water for very high molar ratio of H₂O to SO₂
272 in the atmosphere. As a result, $\delta^{18}\text{O}$ value of SO₂ is dynamically controlled by $\delta^{18}\text{O}$ value of water and
273 $\delta^{18}\text{O}$ value of SO₂ has no obvious effect on $\delta^{18}\text{O}$ value of sulfate produced from different oxidation
274 pathways. Meanwhile, sulfate is very stable with respect to O atom exchange with ambient water.
275 Consequently, $\delta^{18}\text{O}$ can be adopted to distinguish SO₂ oxidation processes due to that $\delta^{18}\text{O}$ value of
276 product sulfate reflected the distinctive signals of different oxidants.

277 We simulatively studied SO₂ heterogeneous oxidation by H₂O₂ and Fe³⁺/O₂ in the laboratory, which
278 aims to make clear the relationship of $\delta^{18}\text{O}$ values between product sulfate and [three kinds of](#) water at
279 10 °C. It can be observed from Fig. 7 that $\delta^{18}\text{O}$ value of sulfate was linearly dependent on $\delta^{18}\text{O}$ value of
280 water, and the slope of linear curve for H₂O₂ oxidation approximates a ratio of 0.43, indicating that the

281 isotopy of about two of four oxygen atoms in sulfate was controlled by $\delta^{18}\text{O}$ value of water. The other
 282 two oxygen atoms were from H_2O_2 molecules, whose O-O bond remained intact during SO_2 oxidation.
 283 In addition, we noted from Fig. 7 that the slope of linear curve for $\text{Fe}^{3+}/\text{O}_2$ oxidation was about 0.65,
 284 which represented that the isotopy of about three of four oxygen atoms in sulfate was related to $\delta^{18}\text{O}$
 285 value of water. A 3/4 control of sulfate oxygens by water is also characteristic of heterogeneous
 286 oxidation mechanisms in which HSO_3^- isotopically equilibrated with water prior to significant
 287 oxidation to SO_4^{2-} . The other one oxygen atom in sulfate was from O_2 . The higher slope suggested a
 288 higher dependence of $\delta^{18}\text{O}$ value of sulfate on $\delta^{18}\text{O}$ value of water during SO_2 heterogeneous oxidation
 289 by $\text{Fe}^{3+}/\text{O}_2$. The discrepancy of the slopes for different SO_2 heterogeneous oxidation processes provides
 290 us a potential method to distinguish SO_2 oxidation pathways.



291
 292 **Fig.7.** The correlation of $\delta^{18}\text{O}$ values between H_2O and sulfate from SO_2 oxidation by H_2O_2 and
 293 $\text{Fe}^{3+}/\text{O}_2$, respectively.

294 3.5 $\delta^{18}\text{O}$ - SO_4^{2-} values in $\text{PM}_{2.5}$ and SO_2 main oxidation pathways

295 As depicted in Fig. 8, $\delta^{18}\text{O}$ values of sulfate in $\text{PM}_{2.5}$ ranged from 11.09 to 12.93‰ with an average
 296 and standard deviation of $12.35 \pm 0.68\%$. $\delta^{18}\text{O}$ values of sulfate focused on a narrow scope except those
 297 on 5 and 22 Dec.. It should be pointed out $\delta^{18}\text{O}$ value of secondary sulfate was a comprehensive result
 298 from different SO_2 oxidation processes. Sulfate in $\text{PM}_{2.5}$ usually consisted of primary sulfate and
 299 secondary sulfate. The $\delta^{18}\text{O}$ value of primary sulfate is about 38 ‰ (Holt and Kumar, 1984), which is
 300 significantly higher than those of secondary sulfate. The contribution of primary and secondary sulfate

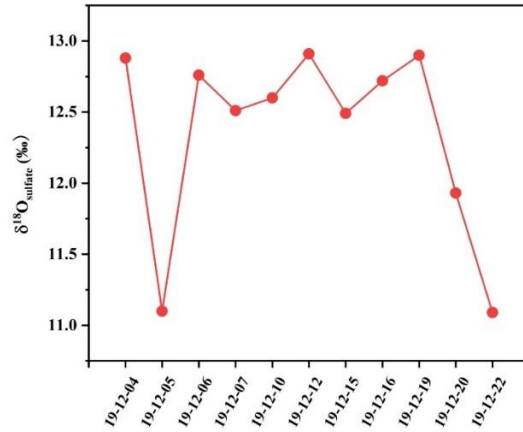


Fig.8. $\delta^{18}\text{O}$ values of sulfate in $\text{PM}_{2.5}$ during the sampling period.

带格式的: 居中, 缩进: 首行缩进: 0 字符

in the atmosphere can be calculated by oxygen isotope mass equilibrium equation (4) (Ben et al., 1982).

$$\delta^{18}\text{O}_{\text{PM}_{2.5}} = \delta^{18}\text{O}_{\text{PS}} \times (1 - f_{\text{SS}}) + \delta^{18}\text{O}_{\text{SS}} \times f_{\text{SS}} \quad (4)$$

where $\delta^{18}\text{O}_{\text{PM}_{2.5}}$, $\delta^{18}\text{O}_{\text{PS}}$ and $\delta^{18}\text{O}_{\text{SS}}$ mean $\delta^{18}\text{O}$ values of $\text{PM}_{2.5}$, primary sulfate and secondary sulfate, respectively; f_{SS} is the contribution of secondary sulfate in $\text{PM}_{2.5}$.

It is noteworthy from Fig. 9 that there exists a linear relationship between $\delta^{18}\text{O}$ values in water and secondary sulfate from different SO_2 oxidation pathways, and this can be described by the equations (5)-(7), where the value of $\delta^{18}\text{O}_{\text{water}}$ is about -6.2‰ in Nanjing. As discussed above, secondary sulfate was mainly ascribed to SO_2 homogeneous oxidation by OH radicals and heterogeneous oxidation by H_2O_2 and $\text{Fe}^{3+}/\text{O}_2$. Therefore, $\delta^{18}\text{O}_{\text{SS}}$ value in equation (4) can be obtained based on equations (5)-(7) respectively. As a result, the average contribution of primary and secondary sulfate in $\text{PM}_{2.5}$ are presented in Table 1. It can be observed that the majority of sulfate in $\text{PM}_{2.5}$ was secondary sulfate, which appears to constitute from 79.9 to 86.2% of total sulfate during the sampling period. It is admirable to quantitatively describe these formation pathways of secondary sulfate in $\text{PM}_{2.5}$.

带格式的: 下标

$$\delta^{18}\text{O}_{\text{sulfate}} = 0.06 \times \delta^{18}\text{O}_{\text{water}} + 3.8 \text{‰ (PS)} \quad (\text{Holt and Kumar, 1984}) \quad (5)$$

$$\delta^{18}\text{O}_{\text{SS}} = 0.69 \times \delta^{18}\text{O}_{\text{water}} + 9.5 \text{‰ (OH)} \quad (\text{Holt and Kumar, 1984}) \quad (5)$$

$$\delta^{18}\text{O}_{\text{SS}} = 0.65 \times \delta^{18}\text{O}_{\text{water}} + 10.6 \text{‰ (Fe}^{3+}/\text{O}_2) \quad (\text{this study}) \quad (6)$$

$$\delta^{18}\text{O}_{\text{SS}} = 0.43 \times \delta^{18}\text{O}_{\text{water}} + 12.5 \text{‰ (H}_2\text{O}_2) \quad (\text{this study}) \quad (7)$$

带格式的: 字体: 10 磅

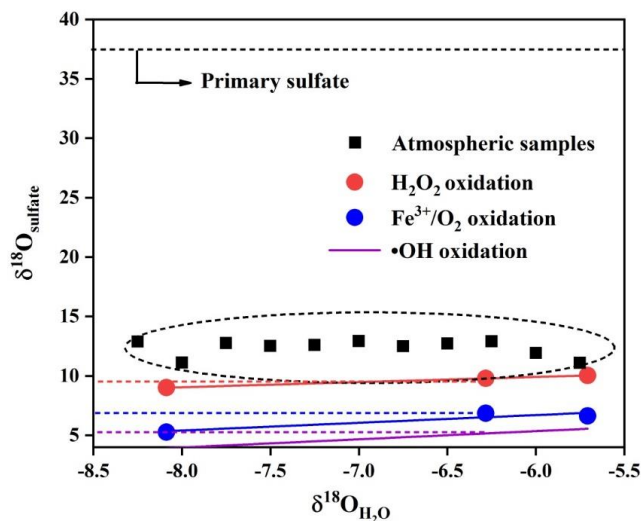


Fig.9. The correlation between $\delta^{18}\text{O}$ values in water and sulfate in $\text{PM}_{2.5}$.

Table 1 The [average](#) contribution of primary sulfate and secondary sulfate in $\text{PM}_{2.5}$.

Sampling time	Primary sulfate (%)	Secondary sulfate (%)
4 Dec.	10.9-23.7 19.7	76.3-89.1 80.3
5 Dec.	4.6-18.2 13.9	81.8-95.4 86.1
6 Dec.	10.6-23.3 19.3	76.7-89.4 80.7
7 Dec.	9.6-22.5 18.4	77.5-90.4 81.6
10 Dec.	10.0-22.8 18.7	77.2-90.0 81.3
12 Dec.	11.1-23.8 20.0	76.2-89.9 80.0
15 Dec.	9.6-22.5 18.4	77.5-90.4 81.6
16 Dec.	11.9-23.6 20.1	76.4-88.1 79.9
19 Dec.	11.0-23.7 19.7	76.3-89.0 80.3
20 Dec.	7.7-20.8 16.7	79.2-92.3 83.3
22 Dec.	4.5-18.1 13.8	79.1-95.5 86.2

According to the percentages of SO_2 heterogeneous and homogeneous oxidation to sulfate in Fig.6 and the average contributions of primary sulfate and secondary sulfate in $\text{PM}_{2.5}$ in Table 1, we can further calculate the ratios of different SO_2 oxidation pathways at 10 °C via oxygen isotope mass

329 equilibrium equations (8)-(10), and the corresponding results are depicted in Table 2.

$$330 \quad \delta^{18}\text{O}_{\text{PM}_{2.5}} = \delta^{18}\text{O}_{\text{PS}} \times f_{\text{PS}} + (\delta^{18}\text{O}_{\text{SS-OH}} \times f_{\text{SS-OH}} + \delta^{18}\text{O}_{\text{SS-Fe}^{3+}/\text{O}_2} \times f_{\text{SS-Fe}^{3+}/\text{O}_2} + \delta^{18}\text{O}_{\text{SS-H}_2\text{O}_2} \times f_{\text{SS-H}_2\text{O}_2}) \times f_{\text{SS}} \quad (8)$$

$$331 \quad f_{\text{PS}} + f_{\text{SS}} = 1 \quad (9)$$

$$332 \quad f_{\text{SS-OH}} + f_{\text{SS-Fe}^{3+}/\text{O}_2} + f_{\text{SS-H}_2\text{O}_2} = 1 \quad (10)$$

333 where $\delta^{18}\text{O}_{\text{PM}_{2.5}}$ and $\delta^{18}\text{O}_{\text{PS}}$ are $\delta^{18}\text{O}$ values of total sulfate and primary sulfate in $\text{PM}_{2.5}$; $\delta^{18}\text{O}_{\text{SS-OH}}$,
 334 $\delta^{18}\text{O}_{\text{SS-Fe}^{3+}/\text{O}_2}$ and $\delta^{18}\text{O}_{\text{SS-H}_2\text{O}_2}$ are $\delta^{18}\text{O}$ values of secondary sulfate from SO_2 oxidation by OH radicals,
 335 $\text{Fe}^{3+}/\text{O}_2$ and H_2O_2 , respectively; f_{PS} and f_{SS} are the contribution of primary and secondary sulfate; $f_{\text{SS-OH}}$,
 336 $f_{\text{SS-Fe}^{3+}/\text{O}_2}$ and $f_{\text{SS-H}_2\text{O}_2}$ are the ratios of secondary sulfate from SO_2 oxidation by OH radicals, $\text{Fe}^{3+}/\text{O}_2$ and
 337 H_2O_2 , respectively.

338 Unlike heavily polluted days with reduced solar irradiation, the photochemical reactivity can remain
 339 high in clean days during the observation period because of relatively intense solar irradiation. As a
 340 result, some photochemical reactive species such as OH radicals and H_2O_2 are deemed to be the major
 341 oxidants for sulfate formation. [Generally, \$\text{H}_2\text{O}_2\$ production in the relatively clean atmosphere is](#)
 342 [ascribed to self-reaction of \$\text{HO}_2\$ radicals that mainly come from the reactions of OH radicals with CO](#)
 343 [and volatile organic compounds.](#) It is observed from Table 2 that the ratios of SO_2 oxidation by OH
 344 radicals ranged from 38 to 68% with an average and standard deviation at $48 \pm 9.7\%$. The ratio reached
 345 the maximum of 68% on 16 Dec., which is mainly ascribed to the highest temperature of 15°C during
 346 the sampling period. The photochemical reactions are favorable for producing more OH radicals. In
 347 contrast, the ratio of SO_2 oxidation by OH radicals decreased to the minimum of 38% on 6 Dec. due to
 348 the low temperature.

349 **Table 2** The ratios of SO_2 different oxidation pathways to sulfate.

Time	$f_{\text{SS-OH}}$	$f_{\text{SS-H}_2\text{O}_2}$	$f_{\text{SS-Fe}^{3+}/\text{O}_2}$	$f_{\text{SS-H}_2\text{O}_2} / (f_{\text{SS-H}_2\text{O}_2} + f_{\text{SS-Fe}^{3+}/\text{O}_2})$ (%)
4 Dec.	0.45	0.27	0.28	49.1
5 Dec.	0.39	0.24	0.37	39.3
6 Dec.	0.38	0.24	0.38	38.7
7 Dec.	0.41	0.25	0.34	42.3
10 Dec.	0.45	0.27	0.28	49.1
12 Dec.	0.59	0.30	0.11	73.2
15 Dec.	0.44	0.26	0.30	46.5

带格式的: 非上标/下标

带格式的: 字体: (中文) 宋体, 10 磅

带格式的: 字体: (中文) 宋体, 10 磅

带格式的: 字体: (中文) 宋体, 10 磅

带格式表格

16 Dec.	0.68	0.26	0.06	81.2
19 Dec.	0.40	0.25	0.35	41.6
20 Dec.	0.54	0.31	0.15	67.4
22 Dec.	0.56	0.32	0.12	72.7

350

351 It is known that SO₂ oxidation by H₂O₂ and Fe³⁺/O₂ are the most important pathways during SO₂
352 heterogeneous oxidation. It can be observed from table 2 that the percentage of sulfate from SO₂
353 oxidation by H₂O₂ in secondary sulfate from SO₂ heterogeneous oxidation changed from 38.7 to 81.2%
354 with an average and standard deviation at 54.6±15.7%, indicating that SO₂ oxidation by H₂O₂
355 predominated during SO₂ heterogeneous oxidation. In addition, there existed an obviously positive
356 correlation between the ratios of SO₂ oxidation by H₂O₂ and OH radicals, which was chiefly attributed
357 to the photochemical reactions. The relatively strong solar irradiation on 16 Dec. resulted in the
358 maximum ratio of 81.2% about H₂O₂ oxidation in SO₂ heterogeneous reactions. The sampling site is
359 close to Nanjing steel plant. As companion emitters, Fe³⁺ are present in much higher concentrations
360 than that in other areas. It is believed that SO₂ oxidation by O₂ in the presence of Fe³⁺ was not negligent
361 in the areas where the concentrations of SO₂ and Fe³⁺ were high. This inevitably resulted in high SO₂
362 oxidation ratio by Fe³⁺/O₂ in SO₂ heterogeneous oxidation processes.

363 4 Conclusions

364 There was no serious PM_{2.5} pollution during the sampling period. The secondary sulfate constitutes
365 from about 79.9 to 86.2% of total sulfate in PM_{2.5}. SO₂ oxidation by O₃ and NO₂ played an
366 insignificant role in sulfate formation. The secondary sulfate was mainly ascribed to SO₂ homogeneous
367 oxidation by OH radicals and heterogeneous oxidation by H₂O₂ and Fe³⁺/O₂. Compared to
368 homogeneous oxidation, SO₂ heterogeneous oxidation was generally dominant with an average
369 contribution of 51.6%. SO₂ oxidation by H₂O₂ predominated in SO₂ heterogeneous oxidation reactions
370 and the average ratio of which reached 54.6%. Consequently, sulfur and oxygen isotopes can be used to
371 gain an insight into sulfate formation. Sulfur isotopic compositions in SO₂ and sulfate were
372 simultaneously measured to quantify the contributions of SO₂ homogeneous and heterogeneous
373 oxidation. Combining field observations of oxygen isotope in the atmosphere with the linear
374 relationships of δ¹⁸O values between H₂O and sulfate from different SO₂ oxidation processes can obtain

带格式的: 字体: 10 磅

带格式的: 字体: 10 磅

带格式的: 字体: 10 磅

带格式的: 字体: 10 磅

375 | [an increased understanding of specific sulfate formation pathways. This study is favorable for deeply](#)
376 | [investigating sulfur cycle in the atmosphere.](#)

377

378 **Author contribution**

379 Ziyang Guo carried out the experiment and wrote the original draft. Keding Lu designed the
380 methodology and administrated the project. Pengxiang Qiu and Mingyi Xu performed the data
381 collection. Zhaobing Guo instructed the experiment and revised the paper.

382 **Competing interests**

383 The authors declare that they have no competing interest that can influence the work reported in this
384 paper.

385 **Acknowledgement**

386 We gratefully acknowledge the financial supports from the National Natural Science Foundation of
387 China (Nos. 41873016, 51908294, and 21976006), the National Science Fund for Distinguished Young
388 Scholars (No. 22325601).

389

390

391 **References**

- 392 Abbatt, J. P. D., Benz, S., Cziczo, D. J., Kanji, Z., Lohmann, U., and Mohler, O.: Solid ammonium
393 sulfate aerosols as ice nuclei: a pathway for cirrus cloud formation, *Science*, 313, 1770-1773,
394 <https://doi.org/10.1126/science.1129726>, 2006.
- 395 Ben, D. H., Romesh, K., and Paul, T. C.: Primary Sulfates in Atmospheric Sulfates: Estimation by
396 Oxygen Isotope Ratio Measurements, *Science*, 217, 51-53, <https://doi.org/10.1126/science.217.4554.51>,
397 1982.
- 398 Brüggemann, M., Riva, M., Perrier, S., Poulain, L., George, C., and Herrmann, H.: Overestimation of
399 Monoterpene Organosulfate Abundance in Aerosol Particles by Sampling in the Presence of SO₂,
400 *Environ. Sci. Technol. Lett.*, 8, 206-211, <https://doi.org/10.1021/acs.estlett.0c00814>, 2021.
- 401 Cheng, Y. F., Zheng, G. J., Wei, C., Mu, Q., Zheng, B., Wang, Z. B., Gao, M., Zhang, Q., He, K. B.,
402 Carmichael, G., Pöschl, U., and Su, H.: Reactive Nitrogen Chemistry in Aerosol Water as a Source of
403 Sulfate during Haze Events in China, *Sci. Adv.*, 2, e1601530, <https://doi.org/10.1126/sciadv.1601530>,
404 2016.
- 405 Gao, J., Wei, Y., Zhao, H., Liang, D., Feng, Y., and Shi, G.: The role of source emissions in sulfate
406 formation pathways based on chemical thermodynamics and kinetics model, *Sci. Total. Environ.*, 851,
407 158104, <https://doi.org/10.1016/j.scitotenv.2022.158104>, 2022.
- 408 Guo, Z. B., Shi, L., Chen, S. L., Jiang, W. J., Wei, Y., Rui, M. L., and Zeng, G.: Sulfur isotopic
409 fractionation and source apportionment of PM_{2.5} in Nanjing region around the second session of the
410 Youth Olympic Games, *Atmos. Res.*, 174-175, 9-17, <https://doi.org/10.1016/j.atmosres.2016.01.011>,
411 2016.
- 412 Guo, Z. Y., Guo, Q. J., Chen, S. L., Zhu, B., Zhang, Y., Yu, J., and Guo, Z. B.: Study on pollution
413 behavior and sulfate formation during the typical haze event in Nanjing with water soluble inorganic
414 ions and sulfur isotopes, *Atmos. Res.*, 217, 198-207, <https://doi.org/10.1016/j.atmosres.2018.11.009>,
415 2019.
- 416 Han, X. K., Guo, Q. J., Liu, C. Q., Fu, P. Q., Strauss, H., Yang, J., Jian, H., Wei, L., Hong, R., Peters,
417 M., Wei, R. F., and Tian, L.: Using stable isotopes to trace sources and formation processes of sulfate
418 aerosols from Beijing, China, *Sci. Rep.*, 6, 29958, <https://doi.org/10.1038/srep29958>, 2016.
- 419 Han, X. K., Guo, Q. J., Strauss, H., Liu, C. Q., Hu, J., Guo, Z. B., Wei, R. F., Peters, M., Tian, L., and

420 Kong, J.: Multiple Sulfur Isotope Constraints on Sources and Formation Processes of Sulfate in Beijing
421 PM_{2.5} Aerosol, Environ. Sci. Technol., 51, 7794-7803, <https://doi.org/10.1021/acs.est.7b00280>, 2017.

422 Harris, E., Sinha, B., Hoppe, P., and Ono, S.: High-precision measurements of ³³S and ³⁴S fractionation
423 during SO₂ oxidation reveal causes of seasonality in SO₂ and sulfate isotopic composition, Environ. Sci.
424 Technol., 47, 12174-12183, <https://doi.org/10.1021/es402824c>, 2013.

425 Harris, E., Sinha, B., Hoppe, P., Crowley, J. N., Ono, S., and Foley, S.: Sulfur isotope fractionation
426 during oxidation of sulfur dioxide: gas-phase oxidation by OH radicals and aqueous oxidation by H₂O₂,
427 O₃ and iron catalysis, Atmos. Chem. Phys., 12, 407-424, <https://doi.org/10.5194/acp-12-407-2012>,
428 2012.

429 He, P. Z., Alexander, B., Geng, L., Chi, X. Y., Fan, S. D., Zhan, H. C., Kang, H., Zheng, G. J., Cheng, Y.
430 F., Su, H., Liu, C., and Xie, Z. Q.: Isotopic constraints on heterogeneous sulfate production in Beijing
431 haze, Atmos. Chem. Phys., 18, 5515-5528, <https://doi.org/10.5194/acp-18-5515-2018>.

432 He, X., Wu, J. J., Ma, Z. C., Xi, X., and Zhang, Y. H.: NH₃-promoted heterogeneous reaction of SO₂ to
433 sulfate on α-Fe₂O₃ particles with coexistence of NO₂ under different relative humidities, Atmos.
434 Environ., 262, 118622, <https://doi.org/10.1016/j.atmosenv.2021.118622>, 2021.

435 [Holt, B.D. and Kumar R.: Oxygen-18 study of high-temperature air oxidation of SO₂. Atmos. Environ.,](#)
436 [18, 2089-2094, https://doi.org/10.1016/0004-6981\(84\)90194-X, 1984.](#)

437 Huang, R. J., Zhang, Y., Bozzetti, C., Ho, K. F., Cao, J. J., Han, Y., Daellenbach, K. R., Slowik, J. G.,
438 Platt, S. M., Canonaco, F., Zotter, P., Wolf, R., Pieber, S. M., Bruns, E. A., Crippa, M., Ciarelli, G.,
439 Piazzalunga, A., Schwikowski, M., Abbaszade, G., Schnelle-Kreis, J., Zimmermann, R., An, Z., Szidat,
440 S., Baltensperger, U., El Haddad, I., and Prevot, A. S.: High secondary aerosol contribution to
441 particulate pollution during haze events in China, Nature, 514, 218-222,
442 <https://doi.org/10.1038/nature13774>, 2014.

443 Kuang, B., Zhang, F., Shen, J., Shen, Y., Qu, F., Jin, L., Tang, Q., Tian, X., and Wang, Z.: Chemical
444 characterization, formation mechanisms and source apportionment of PM_{2.5} in north Zhejiang Province:
445 The importance of secondary formation and vehicle emission, Sci. Total. Environ., 851, 158206,
446 <https://doi.org/10.1016/j.scitotenv.2022.158206>, 2022.

447 Li, J. H. Y., Zhang, Y. L., Cao, F., Zhang, W., and Michalski, G.: Stable Sulfur Isotopes Revealed a
448 Major Role of Transition-Metal Ion-Catalyzed SO₂ Oxidation in Haze Episodes, Environ. Sci. Technol.,

带格式的: 下标

域代码已更改

带格式的: 超链接, 字体: (默认)
Times New Roman, (中文) 等线, 字
体颜色: 自动设置

449 54, 2626-2634, <https://doi.org/10.1021/acs.est.9b07150>, 2020.

450 Lin, Y. C., Yu, M., Xie, F., and Zhang, Y.: Anthropogenic Emission Sources of Sulfate Aerosols in
451 Hangzhou, East China: Insights from Isotope Techniques with Consideration of Fractionation Effects
452 between Gas-to-Particle Transformations, *Environ. Sci. Technol.*, 56, 3905-3914.
453 <https://doi.org/10.1021/acs.est.1c05823>, 2022.

454 Liu, M. X., Song, Y., Zhou, T., Xu, Z. Y., Yan, C. Q., Zheng, M., Wu, Z. J., Hu, M., Wu, Y. S., and Zhu,
455 T.: Fine particle pH during severe haze episodes in northern China, *Geophys. Res. Lett.*, 44, 5213-5221,
456 <https://doi.org/10.1002/2017GL073210>, 2017.

457 Liu, T., Clegg, S. L., Abbatt, J. P. D.: Fast oxidation of sulfur dioxide by hydrogen peroxide in
458 deliquesced aerosol particles, *Proc. Natl Acad. Sci. USA.*, 117, 1354-1359,
459 <https://doi.org/10.1073/pnas.1916401117>, 2020.

460 Liu, Y. Y., Wang, T., Fang, X. Z., Deng, Y., Cheng, H. Y., Nabi, I., and Zhang, L.: Brown carbon: An
461 underlying driving force for rapid atmospheric sulfate formation and haze event, *Sci. Total. Environ.*,
462 734, 139415, <https://doi.org/10.1016/j.scitotenv.2020.139415>, 2020.

463 Meng, X., Hang, Y., Lin, X., Li, T. T., Wang, T. J., Cao, J. J., Fu, Q. Y., Dey, S., Huang, K., Liang, F. C.,
464 Kan, H. D., Shi, X. M., and Liu, Y.: A satellite-driven model to estimate long-term particulate sulfate
465 levels and attributable mortality burden in China, *Environ. Int.*, 171, 107740,
466 <https://doi.org/10.1016/j.envint.2023.107740>, 2023.

467 Oh, S. H., Park, K., Park, M., Song, M., Jang, K. S., Schauer, J. J., Bae, G. N., and Bae, M. S.:
468 Comparison of the sources and oxidative potential of PM_{2.5} during winter time in large cities in China
469 and South Korea, *Sci. Total. Environ.*, 859, 160369, <https://doi.org/10.1016/j.scitotenv.2022.160369>,
470 2023.

471 Ramanathan, V., Crutzen, P. J., Kiehl, J. T., and Rosenfeld, D.: Aerosols, climate, and the hydrological
472 cycle, *Science*, 294, 2119-2124, <https://doi.org/10.1126/science.1064034>, 2001.

473 Seinfeld, J. H. and Pandis, S. N.: Atmospheric Chemistry and Physics: From Air Pollution to Climate
474 Change, *Phys. Today*, 51, 88-90, <https://doi.org/10.1063/1.882420>, 1998.

475 Shao, J., Chen, Q., Wang, Y., Lu, X., He, P., Sun, Y., Shah, V., Martin, R. V., Philip, S., Song, S., Zhao,
476 Y., Xie, Z., Zhang, L., and Alexander, B.: Heterogeneous sulfate aerosol formation mechanisms during
477 wintertime Chinese haze events: air quality model assessment using observations of sulfate oxygen

478 isotopes in Beijing, *Atmos. Chem. Phys.*, 19, 6107-6123, <https://doi.org/10.5194/acp-19-6107-2019>,
479 2019.

480 Tanaka, N., Rye, D. M., Xiao, Y., and Lassaga, A. C.: Use of stable sulfur isotope systematic for
481 evaluating oxidation reaction pathways and in-cloud scavenging of sulfur dioxide in the atmosphere,
482 *Geophys. Res. Lett.*, 21, 1519-1522, <https://doi.org/10.1029/94GL00893>, 1994.

483 Wang, G. H., Zhang, R. Y., Gomez, M. E., Yang, L. X., Levy Zamora, M., Hu, M., Lin, Y., Peng, J. F.,
484 Guo, S., Meng, J. J., Li, J. J., Cheng, C. L., Hu, T. F., Ren, Y. Q., Wang, Y. S., Gao, J., Cao, J. J., An, Z.
485 S., Zhou, W. J., Li, G. H., Wang, J. Y., Tian, P. F., Marrero-Ortiz, W., Secrest, J., Du, Z. F., Zheng, J.,
486 Shang, D. J., Zeng, L. M., Shao, M., Wang, W. G., Huang, Y., Wang, Y., Zhu, Y. J., Li, Y. X., Hu, J. X.,
487 Pan, B., Cai, L., Cheng, Y. T., Ji, Y. M., Zhang, F., Rosenfeld, D., Liss, P. S., Duce, R. A., Kolb, C. E.,
488 and Molina, M. J.: Persistent sulfate formation from London Fog to Chinese haze, *Proc. Natl. Acad. Sci.*
489 *U.S. A.*, 113, 13630-13635, <https://doi.org/10.1073/pnas.1616540113>, 2016.

490 Wang, W., Liu, M., Wang, T., Song, Y., and Ge, M.: Sulfate formation is dominated by
491 manganese-catalyzed oxidation of SO₂ on aerosol surfaces during haze events, *Nature Communications*,
492 12, 1993, <https://doi.org/10.1038/s41467-021-22091-6>, 2021.

493 Xue, J., Yuan, Z., Griffith, S. M., Yu, X., Lau, A. K. H., and Yu, J. Z.: Sulfate Formation Enhanced by a
494 Cocktail of High NO_x, SO₂, Particulate Matter, and Droplet pH during Haze-Fog Events in Megacities
495 in China: An Observation-Based Modeling Investigation, *Environ. Sci. Technol.*, 50, 7325-7334,
496 <https://doi.org/10.1021/acs.est.6b00768>, 2016.

497 Xue, J., Yuan, Z., Yu, J. Z., and Lau, A. K. H.: An Observation-Based Model for Secondary Inorganic
498 Aerosols, *Aerosol Air Qual. Res.*, 14, 862-878, <https://doi.org/10.4209/aaqr.2013.06.0188>, 2014.

499 Yang, T., Xu, Y., Ye, Q., Ma, Y. J., Wang, Y. C., Yu, J. Z., Duan, Y. S., Li, C. X., Xiao, H. W., Li, Z. Y.,
500 Zhao, Y., and Xiao, H. Y.: Spatial and diurnal variations of aerosol organosulfates in summertime
501 Shanghai, China: potential influence of photochemical processes and anthropogenic sulfate pollution,
502 *Atmos. Chem. Phys.*, 23, 13433-13450, <https://doi.org/10.5194/acp-23-13433-2023>, 2023.

503 Ye, C., Liu, P. F., Ma, Z. B., Xue, C. Y., Zhang, C. L., Zhang, Y. Y., Liu, J. F., Liu, C. T., Sun, X., and
504 Mu, Y. J.: High H₂O₂ Concentrations Observed during Haze Periods during the Winter in Beijing:
505 Importance of H₂O₂ Oxidation in Sulfate Formation, *Environ. Sci. Technol. Lett.*, 5, 757-763,
506 <https://doi.org/10.1021/acs.estlett.8b00579>, 2018.

507 Zhang, R., Sun, X. S., Shi, A. J., Huang, Y. H., Yan, J., Nie, T., Yan, X., and Li, X.: Secondary
508 inorganic aerosols formation during haze episodes at an urban site in Beijing, China, *Atmos. Environ.*,
509 177, 275-282, <https://doi.org/10.1016/j.jes.2022.01.008>, 2018.

510 Zhang, Y., Bao, F. X., Li, M., Xia, H. L., Huang, D., Chen C. C., and Zhao, J. C.: Photoinduced Uptake
511 and Oxidation of SO₂ on Beijing Urban PM_{2.5}, *Environ. Sci. Technol.*, 54,
512 14868-14876, <https://doi.org/10.1021/acs.est.0c01532>, 2020.